Interactions and Reactions of Sulfur Trioxide, Water, and Ammonia: An ab Initio and Density Functional Theory Study

Laura J. Larson and Fu-Ming Tao*

Department of Chemistry and Biochemistry, California State University, Fullerton, California 92834

Received: November 30, 2000; In Final Form: February 21, 2001

The interactions and reactions of sulfur trioxide (SO_3), ammonia (NH_3), and water (H_2O) are investigated using density functional theory and ab initio molecular orbital theory. Four stable clusters that result from strong intermolecular interactions and reactions of the ternary $SO_3/NH_3/H_2O$ system are considered: $SO_3{\cdot}H_2O{\cdots}NH_3$, $SO_3{\cdot}NH_3{\cdots}H_2O$, $H_2SO_4{\cdots}NH_3$, and $HSO_3NH_2{\cdots}H_2O$. The sulfuric acid−ammonia cluster, $H_2SO_4{\cdots}NH_3$, is found to be the most stable and represents the ultimate fate of the ternary system. However, the zwitterionic sulfamic acid−water cluster, $SO_3{\cdot}NH_3{\cdots}H_2O$, is almost equally stable, indicating that the $SO_3{\cdot}NH_3$ complex may be thermodynamically stable in water vapor. The reaction pathways are studied for the interconversions between the four clusters. Large energy barriers are found between $SO_3{\cdot}NH_3{\cdots}H_2O$ and $SO_3{\cdot}H_2O{\cdots}NH_3$ and between $SO_3{\cdot}NH_3{\cdots}H_2O$ and $HSO_3NH_2{\cdots}H_2O$, and a small barrier is found between $SO_3{\cdot}H_2O{\cdots}NH_3$ and $H_2SO_4{\cdots}NH_3$. As a result, $SO_3{\cdot}H_2O{\cdots}NH_3$ readily converts into the sulfuric acid cluster, $H_2SO_4{\cdots}NH_3$, but conversion of $SO_3{\cdot}NH_3{\cdots}H_2O$ into either $SO_3{\cdot}H_2O{\cdots}NH_3$ or $HSO_3NH_2{\cdots}H_2O$ is kinetically unfavorable. The results suggest that the intermediate fate of SO_3 in the atmosphere depends on the relative concentrations of H_2O and NH_3. In normal atmospheric conditions, where the $SO_3{\cdot}H_2O$ complex forms first due to overwhelmingly larger H_2O mixing ratio, the addition of NH_3 to $SO_3{\cdot}H_2O$ is likely to form $H_2SO_4{\cdots}NH_3$ which evolves into a nucleus of sulfate-based aerosol. On the other hand, in atmospheric conditions where an unusually high NH_3 mixing ratio exists, the $SO_3{\cdot}NH_3$ complex may form first and further stabilize with H_2O.

Introduction

Gas-phase reactions of sulfur trioxide (SO_3), particularly to form sulfuric acid (H_2SO_4), have generated much recent interest. Sulfur trioxide is produced in the atmosphere from the oxidation of sulfur dioxide (SO_2). The latter is released into the atmosphere by both anthropogenic sources, such as coal combustion, and natural sources, such as volcanoes. Dimethyl sulfide (DMS) is also ultimately converted to SO_2 and is subsequently oxidized to SO_3. The formation of H_2SO_4 is important from an atmospheric standpoint as sulfuric acid contributes to acid deposition[1] and is also responsible for the formation of cloud condensation nuclei (CCN).[2] Past theoretical studies[3] indicate that the bimolecular reaction of SO_3 with H_2O to form sulfuric H_2SO_4,

$$SO_3 + H_2O \rightarrow H_2SO_4 \tag{1}$$

has a high energy barrier, approximately 32 kcal mol^{-1}, and is thus unlikely to take place in the atmosphere. However, the reaction involving two water molecules is much more favorable and proceeds through the $SO_3{\cdot}H_2O$ complex:[3−5]

$$SO_3 + H_2O + M \leftrightarrows SO_3{\cdot}H_2O + M \tag{2}$$

$$SO_3{\cdot}H_2O + H_2O \rightarrow H_2SO_4 + H_2O \tag{3}$$

This reaction has a small energy barrier[3] of about 5 kcal mol^{-1}. The energy barrier is completely eliminated when four or more water molecules are present in the reactant cluster.[6]

In addition to the reaction of SO_3 with H_2O, the association of SO_3 with ammonia (NH_3) has drawn much recent attention,

$$SO_3 + NH_3 + M \leftrightarrows SO_3{\cdot}NH_3 + M \tag{4}$$

The effective second-order rate coefficient for reaction 4 is $k = 2 \times 10^{-11}$ cm^3 molecule^{-1} s^{-1} at 1 atm N_2 at 295 K with a free energy change of $\Delta G°_{295} = -10$ kcal mol^{-1}.[7] Ammonia, the only significant base in the atmosphere, is released primarily from animal wastes, NH_3-based fertilizers, and industrial emissions.[8] Recent work of Leopold and co-workers[9−11] suggests that the association of SO_3 with NH_3 in the gas phase results in a zwitterionic isomer ($^{-}SO_3{\cdot}NH_3^{+}$) of neutral sulfamic acid (HSO_3NH_2). This process involves the overlap of the lone-pair orbital on the nitrogen atom with the lowest unoccupied molecular orbital (LUMO) of SO_3,[12] and produces a partial bond between N and S with a calculated covalent bond order of 0.46.[13] Partial electron transfer takes place from N to S, giving rise to the zwitterion $^{-}SO_3{\cdot}NH_3^{+}$, and therefore, the S−N bond represents an electron donor−acceptor (EDA) interaction between SO_3 and NH_3. The staggered conformation of $SO_3{\cdot}NH_3$ is the preferred equilibrium geometry, according to the theoretical studies of Hickling and Woolley.[12]

Compared to the neutral isomer HSO_3NH_2, the $SO_3{\cdot}NH_3$ complex contains a longer S−N bond length (by 0.3 Å),[13] and a much larger dipole moment. The two isomers are comparable in energy in the gas phase, but are separated by a

---

* Author to whom correspondence should be addressed. E-mail: ftao@fullerton.edu.

10.1021/jp004354o CCC: $20.00

large barrier of 28.6 kcal mol^{-1} for the interconversion via a hydrogen 1,3-shift [13]

$$SO_3{\cdot}NH_3 \leftrightarrows HSO_3NH_2 \tag{5}$$

Because the concentration of water in the atmosphere is much larger than that of NH_3 (tropospheric boundary layer mixing ratios of $\sim10^{-2}$ for H_2O and 10^{-11} to 10^{-9} for NH_3),[7] the reaction of SO_3 with water is dominant and is more extensively studied. However, in certain atmospheric conditions, the association of SO_3 with NH_3 may also be significant. The reaction rate constant of $SO_3 + NH_3$ is more than 4 orders of magnitude larger than that of $SO_3 + H_2O$.[14] In addition, the association of SO_3 with NH_3 is much stronger than the association of SO_3 with H_2O. The binding energy of approximately 20 kcal mol^{-1} for $SO_3{\cdot}NH_3$,[7,13] compared with 7.9 kcal mol^{-1} for $SO_3{\cdot}H_2O$,[15] exemplifies this difference. It should be noted that $SO_3{\cdot}H_2O$ is an EDA complex similar to $SO_3{\cdot}NH_3$. Canagaratna et al.[10] compare the two complexes, noting that the experimental intermolecular S−O bond length of the water complex is only about 0.4 Å shorter than a van der Waals bond, while the S−N bond length of the NH_3 complex is shortened by about 0.9 Å relative to the predicted van der Waals distance. This strong attraction between SO_3 and NH_3 is not surprising, considering SO_3 as a strong Lewis acid and NH_3 a Lewis base. The two molecules are expected to form a relatively stable complex in the atmosphere.

The fate of the $SO_3{\cdot}NH_3$ complex in the atmosphere has previously been investigated. Although in the lower troposphere the decomposition of the complex is the major loss process, in the higher troposphere the stability of $SO_3{\cdot}NH_3$ allows it to efficiently form clusters with itself and/or H_2SO_4, or be scavenged by aerosols.[7,16] Moreover, Lovejoy and Hanson[7] suggest that due to the low vapor pressure of sulfamic acid (lower than that of H_2SO_4), $SO_3{\cdot}NH_3$ may play a significant role in particle formation by acting as a precursor for atmospheric aerosol. The studies of Leopold et al.[9] indicate that the most significant changes in the $SO_3{\cdot}NH_3$ complex will occur during the earliest phases of clustering. Canagaratna et al.[10] agree, proposing that the very small cluster level is essential to the understanding of the growth of a sulfamic acid-based particle.

Theoretical studies of Coffman and Hegg[17] suggest that ternary nucleation via $SO_3/H_2O/NH_3$ could represent important sources of particles in the atmosphere, and Lovejoy and Hanson[7] conclude that studies of this three-particle system are needed to evaluate the role of water in sulfamic acid cluster formation. In addition, field studies by Weber et al.[18] at the Mauna Loa Observatory, Hawaii, resulted in atmospheric nucleation rates that were significantly higher than predicated by theory for the H_2SO_4/H_2O system. They suggest that NH_3 may be involved in the nucleation mechanism. A later study by the same group[19] provides the supporting evidence. High concentrations of the smallest measurable ultra-fine particles were detected downwind of a large penguin colony, which provides a significant source of NH_3. Thus, SO_3, H_2O, and NH_3 may collectively play significant roles in atmospheric nucleation and aerosol formation.

This research focuses on the interactions and reactions of SO_3, H_2O, and NH_3 molecules in the gas phase. More specifically, an attempt is made to resolve the following questions. Once the $SO_3{\cdot}H_2O$ complex is formed (reaction 2), would NH_3 aid in the production of H_2SO_4 (reaction 6), or would it simply replace H_2O in the SO_3 complex (reaction 7)?

$$SO_3{\cdot}H_2O + NH_3 \rightarrow H_2SO_4 + NH_3 \tag{6}$$

$$SO_3{\cdot}H_2O + NH_3 \leftrightarrows SO_3{\cdot}NH_3 + H_2O \tag{7}$$

On the other hand, once the $SO_3{\cdot}NH_3$ complex is formed (reaction 4), what is the effect of a water molecule on the complex or does H_2O replace NH_3 in the SO_3 complex (reverse of reaction 7), eventually leading to sulfuric acid (reaction 6)? Is the energy barrier reduced for the production of the neutral isomer of sulfamic acid (reaction 8)? Also, does a H_2O molecule destabilize the neutral isomer relative to $SO_3{\cdot}NH_3$ once it is formed?

$$SO_3{\cdot}NH_3 + H_2O \rightarrow HSO_3NH_2 + H_2O \tag{8}$$

Overall, what is the most stable conformation of the $SO_3/H_2O/NH_3$ system and how easily are all of the conformation isomers converted into the most stable one?

To seek the answers to the above questions, density functional theory (DFT) and ab initio methods are used to study the stable intermolecular complexes that originate from the $SO_3/H_2O/NH_3$ system and the corresponding interconversion reaction pathways. Transition states and energy barriers for the relevant reactions are determined and the most likely reaction pathways in typical atmospheric conditions are discussed.

Theoretical Method

Density functional theory (DFT) and ab initio molecular orbital theory were used to calculate the equilibrium geometry and relative energy of the molecular system at the different configurations considered. The DFT method chosen for this study was the well-established Becke's three-parameter functional[20,21]with the nonlocal correlation provided by Lee, Yang, and Parr (B3LYP).[23] The ab initio method was frozen-core second-order Møller−Plesset perturbation approximation (MP2).[24,25] Both methods are known to be reliable, particularly for calculations of closed-shell stable molecules and hydrogen-bonded complexes.[26,27] Energy calculations were also carried out for the MP2 geometries using CCSD(T) (coupled-cluster theory with singles, doubles, and perturbative triples) method.[28−30] The reasonably large basis sets, 6-31+G* and 6-311++G**,[31−33] were used in all calculations. The results from the two basis sets are nearly the same, and so only the results from the 6-311++G** basis set will be reported.

Molecular clusters were constructed with several distinct initial configurations for geometry optimization. The notations used for the clusters at the different configurations are illustrated as follows. The single dot "•" is used to represent an electron donor−acceptor (EDA) interaction between two molecules in a cluster. For example, the sulfur trioxide−water EDA complex is represented as $SO_3{\cdot}H_2O$. The triple dots "•••" represent weak interactions other than EDA, such as van der Waals force or hydrogen bonding, between two molecules (or two groups of molecules) in a cluster. For example, $SO_3{\cdot}H_2O{\cdots}NH_3$ represents a cluster formed by the association of ammonia to the $SO_3{\cdot}H_2O$ complex via hydrogen bond interactions.

Geometry optimization was initially carried out for the monomers, SO_3, H_2O, and NH_3, as well as for the binary complexes, $SO_3{\cdot}H_2O$ and $SO_3{\cdot}NH_3$. The distinct, stable configurations of the $SO_3/H_2O/NH_3$ ternary cluster system were then considered on the basis of the optimized structures of $SO_3{\cdot}H_2O$ and $SO_3{\cdot}NH_3$. Typically, a stable configuration contains the strongest possible hydrogen bonding or multiple hydrogen-bonding interactions. Specifically, two primary configurations were considered in this study. The first configuration results from the association of NH_3 with $SO_3\cdot H_2O$ via two hydrogen bonds that form a cyclic system. This configuration is denoted as $SO_3\cdot H_2O\cdots NH_3$ and labeled cluster (1a) in all tables and figures. The second configuration results from the association of H_2O with $SO_3\cdot NH_3$, also via two hydrogen bonds that form a cyclic system and is denoted as $SO_3\cdot NH_3\cdots H_2O$ and labeled cluster (2a) in all tables and figures. A third configuration was also considered initially that results as both H_2O and NH_3 interact with SO_3 via EDA interactions (located on either side of the SO_3 plane). However, this configuration was determined to be highly unstable relative to the other two configurations.

Three likely reactions originating from the two primary clusters ($SO_3\cdot H_2O\cdots NH_3$ and $SO_3\cdot NH_3\cdots H_2O$) were considered to form the corresponding product clusters. The $SO_3\cdot H_2O\cdots NH_3$ cluster may react to form $H_2SO_4\cdots NH_3$, a complex of sulfuric acid and ammonia, via reaction 6, and it may also convert into $SO_3\cdot NH_3\cdots H_2O$ via reaction 7. The $SO_3\cdot NH_3\cdots H_2O$ cluster may convert into $SO_3\cdot H_2O\cdots NH_3$ via the reverse of reaction 7 and it may also react to form $HSO_3NH_2\cdots H_2O$, a complex of sulfamic acid and water, via reaction 8. The product clusters $H_2SO_4\cdots NH_3$ and $HSO_3NH_2\cdots H_2O$ are labeled cluster (1b) and (2b), respectively, in all tables and figures.

The transition state structures for the reactions were optimized using the synchronous transit quasi-Newton method[34] and were verified by frequency calculations as well as by intrinsic reaction coordinate (IRC) calculations.[35,36] The transition state from cluster (1a) to (1b) (for reaction 6) is labeled cluster $(1)^\dagger$ while the transition state from cluster (1a) to (2a) (for reaction 7) is labeled cluster $(1-2)^\dagger$. Finally, the transition state separating cluster (2a) and (2b) (reaction 8) is labeled cluster $(2)^\dagger$.

The relative energies of the reactant clusters, transition states, and product clusters were calculated with respect to the isolated SO_3, H_2O, and NH_3 monomers. The relative energies were also calculated at the CCSD(T) level using the MP2 equilibrium geometries. Zero-point energy (ZPE) corrections based on harmonic vibrational frequencies were considered at the B3LYP level to give ZPE-corrected energies, ΔE_0, of the clusters. All B3LYP and MP2 calculations were carried out with the Gaussian 98 program package,[37,38] while CCSD(T) calculations were carried out with the MOLPRO program,[39] on various UNIX workstations.

Results and Discussion

Equilibrium Structures. Table 1 presents the calculated and experimental equilibrium bond lengths, bond angles, and dipole moments of the monomers and binary complexes, and Table 2 presents selected geometric parameters calculated for the ternary reactants, transition states, and products. Figure 1 presents a side view of the 3-dimensional optimized structures of the reactants, transition states, and products, along with the labeling of the atoms for the geometric parameters in Tables 1 and 2. As shown in Tables 1 and 2, the B3LYP and MP2 geometric results are comparable to each other and are in reasonable agreement with experiment. Overall, the equilibrium bond lengths differ by less than 0.1 Å and the bond angles differ by less than 4° between the B3LYP and MP2 results. Discussions in the remainder of this paper will primarily refer to the B3LYP results.

The equilibrium geometries of the $SO_3\cdot H_2O$ and $SO_3\cdot NH_3$ complexes (Table 1) are in close agreement with previously published experimental results. For example, in the $SO_3\cdot H_2O$ cluster, the S−O bond distance of 2.424 Å and O_1−S−O angle of 91.7° are very comparable to the experimental values of 2.432 Å and 92.6° determined by Phillips et al.[40] from microwave spectroscopy. Similarly, for the $SO_3\cdot NH_3$ complex, the S−N bond distance of 2.130 Å and the O_1−S−N angle of 96.6° are comparable to the values of 1.957 Å and 97.6(4)° determined by Canagaratna et al.[10] from microwave spectroscopy. Although there are no experimental results on the ternary clusters for comparisons, it is reasonable to expect that the calculated geometry for the larger clusters is as reliable as that for the small complexes.

TABLE 1: Equilibrium Bond Lengths (Å), Bond Angles (°), and Dipole Moments, μ (D), of the Monomers and Binary Complexes of the $SO_3/H_2O/NH_3$ System Calculated from B3LYP and MP2 Calculations with the 6-311++G Basis Set**

molecule	parameter[a]	expt[b]	B3LYP	MP2
SO_3 (D_{3h})	r(S−O)	1.4198	1.447	1.449
H_2O (C_{2v})	r(O−H)	0.957	0.962	0.959
	∠H−O−H	104.5	105.0	103.5
	μ	1.94	2.16	2.19
NH_3 (C_{3v})	r(N−H)	1.012	1.015	1.014
	∠H−N−H	106.7	107.9	107.2
	μ	1.51	1.69	1.74
$SO_3\cdot H_2O$ (C_s)	r(S−O1)		1.448	1.447
	r(S−O)	2.432	2.424	2.500
	$r(O_1-H_b)$	2.67	2.883	2.996
	$r(O-H_a)$		0.965	0.962
	$r(O-H_b)$		0.965	0.922
	∠O−S−O1	92.6	91.7	90.9
	∠S−O−Hb	103	111.9	115.7
	μ		3.42	3.08
$SO_3\cdot NH_3$ (C_{3v})	$r(N-H_1)$		1.017	1.017
	$r(S-O_1)$		1.453	1.448
	r(S−N)	1.957	2.130	2.123
	$\angle N-S-O_1$	97.6	96.6	96.4
	$\angle S-N-H_1$		109.2	109.8
	μ	6.20	6.00	5.79

[a] Atomic labels are in reference to Figure 1. [b] Experimental values for SO_3 are from the *CRC Handbook of Chemistry and Physics*, 77th ed.; Lide, D. R., Ed.; CRC: Boca Raton, 1996; for NH_3 and H_2O, values are from Huber, K. P.; Herzberg, G. *Molecular Spectra and Molecular Structure, V. Constants of Polyatomic Molecules*; Van Nostrand Reinhold: New York, 1979; for $SO_3\cdot H_2O$, from ref 40, and for $SO_3\cdot NH_3$ from ref 10 and Canagaratna, M.; Ott, M. E.; Leopold, K. R. *Chem. Phys. Lett.* **1997**, *281*, 63.

It is interesting to notice the geometric changes in the EDA units of the ternary clusters $SO_3\cdot H_2O\cdots NH_3$ and $SO_3\cdot NH_3\cdots H_2O$ from the respective binary EDA complexes. The EDA bond distance r(S−O) decreases from 2.424 Å in $SO_3\cdot H_2O$ to 2.157 Å in $SO_3\cdot H_2O\cdots NH_3$. Similarly, the EDA bond distance r(S−N) decreases from 2.130 Å in $SO_3\cdot NH_3$ to 2.030 Å in $SO_3\cdot NH_3\cdots H_2O$. This suggests that the introduction of the third molecule, H_2O or NH_3, to a binary EDA complex effectively enhances the EDA bond strength and therefore stabilizes the EDA complex. It should be pointed out that the decrease in r(S−N) from $SO_3\cdot NH_3$ to $SO_3\cdot NH_3\cdots H_2O$ of 0.10 Å matches the result of Wong et al.[13] who investigated the solvent effect of a polar medium on the structure of $SO_3\cdot NH_3$ using a continuum model with a condensed dielectric medium of $\epsilon = 40.0$.

In addition to the strong EDA bonds in the ternary clusters, hydrogen bonds are present as a result of the addition of a third molecule to the EDA complex. In $SO_3\cdot H_2O\cdots NH_3$, NH_3 forms two hydrogen bonds with the bond distances $r(N-H_a) = 1.664$ Å and $r(H_2-O_2) = 2.397$ Å. Similarly, in $SO_3\cdot NH_3\cdots H_2O$, H_2O forms two hydrogen bonds with the bond distances $r(O-H_1) = 1.872$ Å and $r(H_b-O_1) = 2.009$ Å. The differences in the hydrogen bond distances indicate that the hydrogen bond between NH_3 and H_2O in both of the clusters is much stronger than that between SO_3 and the added NH_3 or H_2O. In $SO_3\cdot H_2O\cdots NH_3$, NH_3 is the acceptor of a proton from H_2O, while, in

TABLE 2: Equilibrium Bond Lengths (Å), Bond Angles (°), and Dipole Moments, μ (D), of the Ternary Clusters of the $SO_3/H_2O/NH_3$ System, Including Transitions States and Possible Products, Calculated from B3LYP and MP2 Calculations with the 6-311++G Basis Set**

	$H_2SO_4\cdots NH_3$		$(1)^\dagger$		$SO_3\cdot H_2O\cdots NH_3$		$(1-2)^\dagger$		$SO_3\cdot NH_3\cdots H_2O$		$(2)^\dagger$		$HSO_3NH_2\cdots H_2O$	
parameter[a]	B3LYP	MP2	B3LYP	MP2	B3LYP	MP2	B3LYP	MP2	B3LYP	MP2	B3LYP	MP2	B3LYP	MP2
$r(N-H_1)$	1.018	1.018	1.016	1.017	1.016	1.016	1.017	1.017	1.033	1.030	1.437	1.421	2.340	2.375
$r(N-H_2)$	1.585	1.606	1.026	1.016	1.019	1.018	1.016	1.017	1.017	1.019	1.020	1.021	1.018	1.018
$r(N-H_a)$	1.016	1.016	1.261	1.226	1.664	1.716	2.001	2.013	3.612	3.623	3.073	3.032	3.647	3.643
$r(S-N)$	3.433	3.382	3.403	3.259	3.678	3.534	3.217	3.068	2.030	2.007	1.828	1.802	1.712	1.692
$r(S-O_1)$	1.450	1.441	1.458	1.457	1.453	1.451	1.447	1.449	1.464	1.458	1.519	1.509	1.598	1.588
$r(S-O)$	1.639	1.629	1.938	1.905	2.157	2.205	3.448	3.688	3.472	3.469	3.077	3.022	3.338	3.295
$r(O_1-H_b)$	3.260	3.240	2.649	2.712	2.814	2.945	2.821	2.808	2.009	2.021	1.352	1.360	0.996	0.991
$r(O-H_1)$	3.926	3.689	3.102	3.055	3.304	3.179	3.229	3.128	1.872	1.878	1.121	1.119	0.969	0.966
$r(O-H_a)$	4.267	3.958	1.235	1.230	1.020	1.002	0.972	0.967	0.962	0.960	0.966	0.965	0.963	0.962
$r(O-H_b)$	0.969	0.968	0.966	0.967	0.965	0.964	0.962	0.960	0.972	0.969	1.109	1.095	1.723	1.718
$\angle N-S-O_1$	62.2	66.8	99.4	85.3	92.0	76.2	93.3	86.3	97.5	97.4	98.1	97.4	99.1	98.8
$\angle S-N-H_1$	74.2	74.5	118.5	108.1	115.5	90.6	143.1	156.4	107.0	108.2	100.4	99.3	97.1	95.8
$\angle O-S-O_1$	104.2	103.8	99.5	99.4	96.7	96.4	68.8	70.2	52.0	52.2	50.2	51.8	52.3	53.4
$\angle S-O-H_b$	109.0	108.1	108.8	108.9	110.5	112.6	81.5	82.4	50.1	50.3	41.2	41.5	34.2	34.5
μ	5.49	5.51	8.77	8.70	5.98	5.12	3.35	3.46	5.34	5.29	6.37	6.11	5.00	4.80

[a] Atomic labels are in reference to Figure 1.

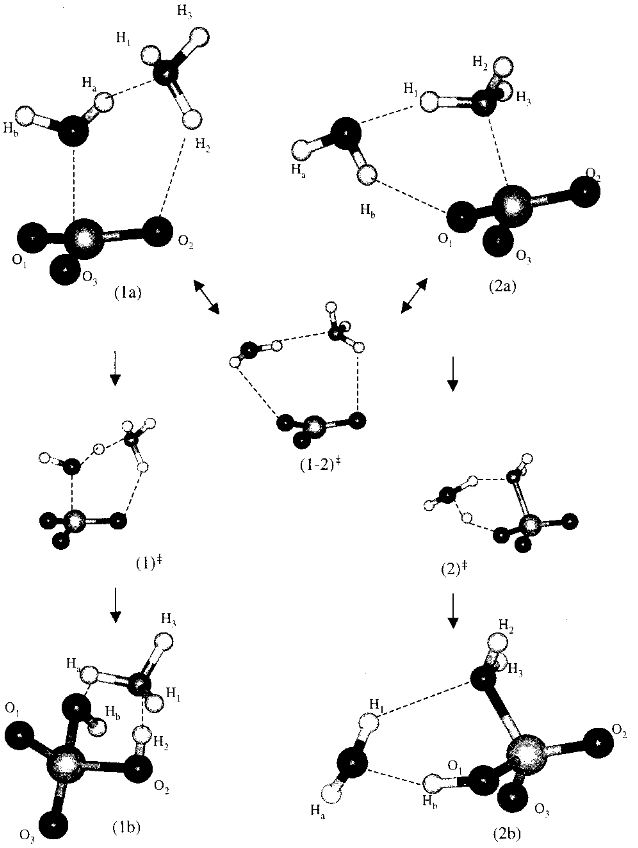

Figure 1. A side view of the optimized 3-D structures of $SO_3\cdot H_2O\cdots NH_3$ (1a), $SO_3\cdot NH_3\cdots H_2O$ (2a), $H_2SO_4\cdots NH_3$ (1b), $HSO_3NH_2\cdots H_2O$ (2b) and the transition states $(1)^\dagger$, $(1-2)^\dagger$, and $(2)^\dagger$.

TABLE 3: Relative Energies, ΔE (kcal mol^{-1}), and Zero-Point Energy Corrected Energies, ΔE_0 (kcal mol^{-1}), of the Binary and Ternary Clusters of the $SO_3/H_2O/NH_3$ System, Including Transition States and Possible Products, from the Indicated Levels of Theory with the 6-311++G Basis Set**

	ΔE			ΔE_0
system/theory	B3LYP	MP2	CCSD(T)	B3LYP
$SO_3\cdot H_2O$	−9.56	−10.00	−10.26	−7.65
$SO_3\cdot NH_3$	−20.24	−19.18	−19.49	−16.86
$H_2SO_4\cdots NH_3$ (1b)	−31.63	−30.19	−32.90	−26.51
$(1)^\dagger$	−22.17	−20.28	−20.41	−18.56
$SO_3\cdot H_2O\cdots NH_3$ (1a)	−24.42	−24.22	−24.21	−19.46
$(1-2)^\dagger$	−10.62	−13.60	−13.70	−7.20
$SO_3\cdot NH_3\cdots H_2O$ (2a)	−32.03	−31.91	−32.58	−25.98
$(2)^\dagger$	−15.80	−15.28	−16.18	−12.49
$HSO_3NH_2\cdots H_2O$ (2b)	−28.54	−29.40	−32.25	−22.87

[a] All values are in reference to isolated SO_3, H_2O, and NH_3 monomers.

$SO_3\cdot NH_3\cdots H_2O$, H_2O is the acceptor of a proton from NH_3. Since NH_3 is a stronger proton acceptor than H_2O, the shorter hydrogen bond is found in $SO_3\cdot H_2O\cdots NH_3$ as noted above. The weakest interaction is between SO_3 and the added NH_3 or H_2O, and therefore it is not surprising that an attempt to find the equilibrium geometry for a third configuration of the ternary cluster failed. Optimization of an initial geometry with H_2O and NH_3 located on either side of the SO_3 plane leads directly to $SO_3\cdot NH_3\cdots H_2O$.

As expected, hydrogen-bond interactions are also present in the product clusters, $H_2SO_4\cdots NH_3$ and $HSO_3NH_2\cdots H_2O$. The $H_2SO_4\cdots NH_3$ cluster contains a very strong hydrogen bond, as shown by the short bond length, $r(N-H_2) = 1.585$ Å. The $HSO_3NH_2\cdots H_2O$ cluster contains a strong hydrogen bond and a weaker secondary hydrogen bond with the bond lengths $r(O-H_b) = 1.723$ Å and $r(O-H_1) = 2.304$ Å, respectively.

The optimized geometry of each transition state cluster generally lies between that of the corresponding reactant and product clusters. The differences between B3LYP and MP2 geometric parameters tend to be larger for the transition state clusters than for the corresponding reactant and product clusters. Frequency calculations and IRC calculations have confirmed the transition state structures. Only one imaginary frequency exists for each of the structures $(1)^\dagger$, $(1-2)^\dagger$, and $(2)^\dagger$.

Energies. Table 3 presents the relative energies ΔE of the reactant, transition state, and product clusters, with respect to the isolated SO_3, H_2O, and NH_3 monomers. The values of ΔE from B3LYP, MP2, and CCSD(T) calculations are in close agreement with each other, in general, differing by less than 2.5 kcal mol^{-1}. The CCSD(T) values appear to be slightly lower than those of the other two methods. Table 3 also lists the PE-corrected energies ΔE_0 of the clusters from B3LYP calculations. Discussions in the remainder of this paper are primarily based on the ZPE-corrected energies.

The two clusters, $SO_3\cdot NH_3\cdots H_2O$ and $H_2SO_4\cdots NH_3$, are found to be the most stable for the $SO_3/H_2O/NH_3$ system, with the former cluster a mere 0.40 kcal mol^{-1} less stable than the

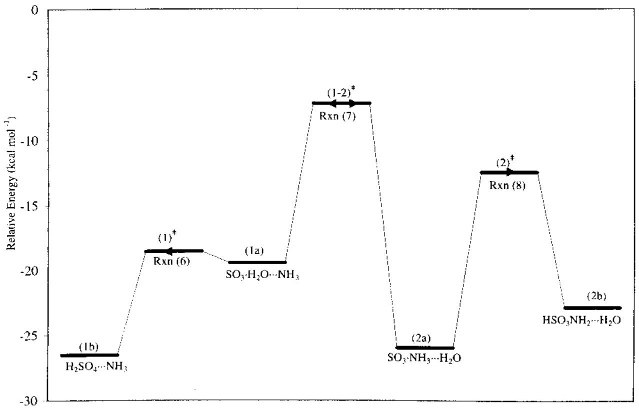

Figure 2. Potential energy profile for the reactions of the $SO_3/H_2O/NH_3$ system from B3LYP calculations with zero-point energy corrections.

latter. Without zero-point energy corrections, however, $SO_3 \cdot NH_3 \cdots H_2O$ is slightly more stable than $H_2SO_4 \cdots NH_3$ at the B3LYP and MP2 levels. These clusters may represent the two likely fates of the $SO_3/H_2O/NH_3$ system, as we shall soon discuss. The stability of $SO_3 \cdot NH_3 \cdots H_2O$ can be attributed to the strong EDA bond in the $SO_3 \cdot NH_3$ unit and to the two hydrogen bonds between $SO_3 \cdot NH_3$ and H_2O. The zwitterionic nature of $SO_3 \cdot NH_3$ also enhances the favorable electrostatic interaction with the polar H_2O. The stability of $H_2SO_4 \cdots NH_3$ can be attributed to the stability of H_2SO_4 with respect to the parent molecules (SO_3 and H_2O), and to the strong hydrogen bond between H_2SO_4 and NH_3.

It is interesting to notice that the $HSO_3NH_2 \cdots H_2O$ cluster is less stable than its parent cluster $SO_3 \cdot NH_3 \cdots H_2O$. In the absence of H_2O, the neutral HSO_3NH_2 isomer is slightly more stable than $SO_3 \cdot NH_3$.[13] The H_2O molecule preferentially stabilizes $SO_3 \cdot NH_3$ over HSO_3NH_2 because of the zwitterionic nature of $SO_3 \cdot NH_3$. The least stable cluster is $SO_3 \cdot H_2O \cdots NH_3$, which is about 6 kcal mol^{-1} higher in energy than either $SO_3 \cdot NH_3 \cdots H_2O$ or $H_2SO_4 \cdots NH_3$.

Reactions. Figure 2 gives an overview of the reaction pathways for the various clusters of the $SO_3/H_2O/NH_3$ system. Starting with the $SO_3 \cdot H_2O \cdots NH_3$ cluster, a small energy barrier of 2.25 kcal mol^{-1} separates $SO_3 \cdot H_2O \cdots NH_3$ from $H_2SO_4 \cdots NH_3$ (reaction 6). The transition state (1)† involves the transfer of a proton from H_2O to NH_3, leading to the appearance of an ammonium cation NH_4^+ (see Figure 1). The reaction is exothermic with a reaction energy of -7.01 kcal mol^{-1}. As a result, the reaction is both kinetically and energetically favorable. The resulting $H_2SO_4 \cdots NH_3$ cluster is a hydrogen-bonded system. Our previous study[41] has shown that an additional water molecule will allow a proton to transfer from H_2SO_4 to NH_3, resulting in an ion-pair system, $HSO_4^- \cdots NH_4^+ \cdots H_2O$.

As just discussed, $SO_3 \cdot H_2O \cdots NH_3$ can easily form $H_2SO_4 \cdots NH_3$. However, the rearrangement of $SO_3 \cdot H_2O \cdots NH_3$ to $SO_3 \cdot NH_3 \cdots H_2O$ is not kinetically favorable. Although this rearrangement is nearly as exothermic as the conversion into $H_2SO_4 \cdots NH_3$, a large energy barrier, 13.80 kcal mol^{-1}, separates $SO_3 \cdot H_2O \cdots NH_3$ from $SO_3 \cdot NH_3 \cdots H_2O$ (reaction 7). Apparently, the strong EDA interaction between SO_3 and H_2O, characterized by the bond distance of $r(S-O) = 2.157$ Å, is not easily disrupted, and the transition state $(1-2)^\dagger$ involving the breakup of such a bond is very unstable. Thus, despite the fact that $SO_3 \cdot NH_3 \cdots H_2O$ is more stable than $SO_3 \cdot H_2O \cdots NH_3$, the large energy barrier prevents the rearrangement of $SO_3 \cdot H_2O \cdots NH_3$ to $SO_3 \cdot NH_3 \cdots H_2O$. In summary, $H_2SO_4 \cdots NH_3$ is the only likely product if the $SO_3/H_2O/NH_3$ system starts initially in the form of $SO_3 \cdot H_2O \cdots NH_3$.

On the other hand, if $SO_3 \cdot NH_3 \cdots H_2O$ were chosen to start, it would not rearrange into $SO_3 \cdot H_2O \cdots NH_3$ [reverse reaction 7] because of a large energy barrier, 21.41 kcal mol^{-1}, and an endothermic energy of reaction, 7.61 kcal mol^{-1}. The $SO_3 \cdot NH_3 \cdots H_2O$ cluster contains a strong EDA interaction unit of $SO_3 \cdot NH_3$. The EDA bond distance in $SO_3 \cdot NH_3 \cdots H_2O$, $r(S-N) = 2.030$ Å, is even shorter than 2.130 Å for the binary $SO_3 \cdot NH_3$ complex. Apparently, the presence of the water molecule has reinforced the EDA interaction within $SO_3 \cdot NH_3$ as discussed earlier. As a result, the rearrangement of $SO_3 \cdot NH_3 \cdots H_2O$ into $SO_3 \cdot H_2O \cdots NH_3$ is both kinetically and energetically unfavorable.

The $SO_3 \cdot NH_3 \cdots H_2O$ might also undergo a hydrogen-shift to form the neutral sulfamic acid/water complex $HSO_3NH_2 \cdots H_2O$ (reaction 8). However, a large energy barrier of 16.13 kcal mol^{-1} makes such a reaction kinetically unfavorable. Furthermore, $SO_3 \cdot NH_3 \cdots H_2O$ is 3.49 kcal mol^{-1} more stable than $HSO_3NH_2 \cdots H_2O$, making this reaction energetically unfavorable as well. As a result, $SO_3 \cdot NH_3 \cdots H_2O$ is likely trapped in an energy-well and stays unreactive.

In summary, if SO_3 is initially complexed with H_2O, the addition of NH_3 to the $SO_3 \cdot H_2O$ complex is likely to result in $H_2SO_4 \cdots NH_3$. On the other hand, if $SO_3 \cdot NH_3$ is initially formed, the addition of water merely forms the $SO_3 \cdot NH_3 \cdots H_2O$ cluster, and the latter is unlikely to convert into either $H_2SO_4 \cdots NH_3$ or $HSO_3NH_2 \cdots H_2O$ without the presence of other species.

Atmospheric Implications. It is apparent that the fate of SO_3 in the atmosphere is highly dependent on whether H_2O or NH_3 is initially associated with SO_3 to form a binary EDA complex. In normal atmospheric conditions, the association of SO_3 with H_2O is at least 100 times faster than the reaction of SO_3 with NH_3 because the concentration of water in the atmosphere is much larger than that of NH_3. More specifically, the tropospheric boundary layer mixing ratio is $\sim 10^{-2}$ for H_2O, compared to 10^{-11} to 10^{-9} for NH_3.[7] If the $SO_3 \cdot H_2O$ complex initially forms, the addition of a single NH_3 molecule to the cluster is likely to result in the formation of $H_2SO_4 \cdots NH_3$. This cluster may form the nuclei of a sulfuric acid-based aerosol.

In heavily polluted atmospheres, however, $[NH_3]/[H_2O]$ can be higher than 10^{-4} and SO_3 may first react with NH_3.[14] Shen et al.[14] propose that if SO_3 first reacts with NH_3, the resulting sulfamic acid reacts with H_2O to form NH_4HSO_4. On the other hand, Lovejoy and Hanson[7] suggest that the $SO_3 \cdot NH_3$ complex ultimately forms HSO_3NH_2. These suggestions are not supported by our results for the interaction and reaction of $SO_3 \cdot NH_3$ with a single water molecule. Instead, our results indicate that the energy barriers to form NH_4HSO_4 and HSO_3NH_2 from the reactions of $SO_3 \cdot NH_3$ with H_2O are reduced but are still very high. It would be interesting to determine the effects of additional water molecules on the interactions and reactions of $SO_3 \cdot NH_3$, particularly on the height of these energy barriers.

The effect of additional water molecules on the $H_2SO_4 \cdots NH_3$ system was investigated previously.[41] The system exists only as a hydrogen-bonded complex in the absence of water. In the presence of a single H_2O molecule, however, the system immediately becomes an ion-pair $HSO_4^- \cdots NH_4^+$ as a result of the transfer of a proton from H_2SO_4 to NH_3. The water molecule assists the proton transfer by stabilizing the ion-pair through favorable electrostatic interactions. In the present study, $SO_3 \cdot H_2O \cdots NH_3$ is shown to readily form $H_2SO_4 \cdot NH_3$ (reaction 6) by overcoming a small energy barrier. The energy barrier for reaction 6 would be eliminated completely if additional solvent water molecules were present in a larger cluster. The final product would be a cluster containing the ion-pair $HSO_4^-\cdots NH_4^+$, a major component of atmospheric aerosols.

It is interesting to notice the significant effect of each individual molecule on the interaction and reaction of the remaining part of a cluster. Most obviously, the energy barrier for $SO_3{\cdot}H_2O$ to form H_2SO_4 is reduced from approximately 32 kcal mol^{-1} (reaction 1)[3] to only 2 kcal mol^{-1} (reaction 6) by the addition of NH_3. Our study shows that NH_3 bridges between the two active sites and shortens the proton-transfer pathway. Alternatively, we may regard NH_3 as a stabilizing solvent molecule. The NH_3 molecule solvates the transferring proton and forms a relatively stable NH_4^+, rather than leaving it as a bare H^+ in the transition state. A similar effect is also found for H_2O on the reaction of $SO_3{\cdot}NH_3$ to form HSO_3NH_2, as the energy barrier decreases from approximately 29 kcal mol^{-1} (reaction 5)[13] to 13.5 kcal mol^{-1} (reaction 8). However, the effect of H_2O is much smaller, which may be attributed to the fact that H_3O^+ is less stable than NH_4^+. These observations exemplify how significant changes may occur in the earliest phases of clustering,[9] and why the very small cluster level is essential to the understanding of particle growth.[10]

The above results support the suggestion by Weber et al.[18] that NH_3 may be involved in the nucleation mechanism of sulfur-based particles. This suggestion is based in part on two separate field studies introduced earlier. First, the observed nucleation rates at the Mauna Loa Observatory, Hawaii, were significantly higher than predicated by theory for the H_2SO_4/H_2O system alone.[18] Second, high concentrations of the smallest measurable ultra-fine particles were detected down-wind of a large penguin colony, which provides a significant source of NH_3.[19] Thus, NH_3 may play a critical role in atmospheric nucleation and particle formation. The present study shows how NH_3 may interact at the molecular level and aid in the formation of nucleation clusters.

Conclusions

The interactions and reactions of SO_3, H_2O, and NH_3 in the gas phase have been studied by density functional theory and ab initio molecular orbital theory. The equilibrium structures and energies were calculated for the stable clusters: $SO_3{\cdot}H_2O\cdots NH_3$, $SO_3{\cdot}NH_3\cdots H_2O$, $H_2SO_4\cdots NH_3$, and $HSO_3NH_2\cdots H_2O$, along with the transition states for their interconversion reactions. The sulfuric acid–ammonia cluster, $H_2SO_4\cdots NH_3$, was found to be the most stable and represents the ultimate fate of the ternary system. However, the $SO_3{\cdot}NH_3\cdots H_2O$ cluster is almost equally stable, indicating that the $SO_3{\cdot}NH_3$ complex may be thermodynamically stable in water vapor. Although the binary complex $SO_3{\cdot}NH_3$ is slightly less stable than isolated neutral sulfamic acid, HSO_3NH_2, the $SO_3{\cdot}NH_3\cdots H_2O$ cluster is considerably more stable than $HSO_3NH_2\cdots H_2O$, indicating the H_2O molecule more favorably stabilizes the zwitterionic $SO_3{\cdot}NH_3$ over the neutral HSO_3NH_2 species.

The reaction pathways were studied for the interconversions between the ternary clusters. A large energy barrier was found between $SO_3{\cdot}H_2O\cdots NH_3$ and $SO_3{\cdot}NH_3\cdots H_2O$ and a small energy barrier was found between $SO_3{\cdot}H_2O\cdots NH_3$ and $H_2SO_4\cdots NH_3$. A large barrier also exists between $SO_3{\cdot}NH_3\cdots H_2O$ and $HSO_3NH_2\cdots H_2O$. As a result, the $SO_3{\cdot}H_2O\cdots NH_3$ cluster readily converts into the sulfuric acid cluster, $H_2SO_4\cdots NH_3$, but conversion of the $SO_3{\cdot}NH_3\cdots H_2O$ cluster into either $SO_3{\cdot}H_2O\cdots NH_3$ or $HSO_3NH_2\cdots H_2O$ is kinetically unfavorable.

The results suggest that the intermediate fate of SO_3 in the atmosphere depends on the relative concentrations of H_2O and NH_3, which determine whether H_2O or NH_3 is initially associated with SO_3. In normal atmospheric conditions, where the $SO_3{\cdot}H_2O$ complex forms first due to overwhelmingly larger H_2O mixing ratio, the addition of NH_3 to $SO_3{\cdot}H_2O$ is likely to result in the formation of $H_2SO_4\cdots NH_3$. This cluster may eventually evolve into a nucleus of sulfate-based aerosol. On the other hand, in atmospheric conditions where an unusually high NH_3 mixing ratio exists, the $SO_3{\cdot}NH_3$ complex may form first and further stabilize with H_2O. The $SO_3{\cdot}NH_3\cdots H_2O$ cluster so formed is kinetically and thermodynamically stable.

It is still not clear from the present study whether or how the $SO_3{\cdot}NH_3\cdots H_2O$ cluster converts into the nuclei of sulfate-based aerosol. The addition of more H_2O molecules may influence the dynamical structure of the $SO_3{\cdot}NH_3$ unit and thereby promote its reactions. It might also be interesting to consider the $SO_3{\cdot}NH_3$ unit in larger clusters with multiple NH_3, SO_3, and/or H_2SO_4 molecules. In fact, Shi et al.[42] investigated the cluster reactions of multiple SO_3 and NH_3 molecules using a time-of-flight reflection mass spectrometer. Lovejoy and Hanson[7] investigated the kinetics and products of the reaction $SO_3 + NH_3$ in the N_2 medium. These studies suggest that both dimerization and the formation of sulfamic acid–sulfuric acid clusters may be low-barrier pathways to cluster formation. Theoretical investigation in this direction is already underway and may provide valuable insights.

Acknowledgment. This work was supported in part by The Petroleum Research Fund (ACS-PRF Grant No. 30399-GB6), The Research Corporation (Award No. CC4121), The Camille and Henry Dreyfus Foundation (Award No. TH-00-028), and College of Natural Sciences & Mathematics and Department of Chemistry & Biochemistry of California State University, Fullerton.

References and Notes

(1) Finalyson-Pitts, B. J.; Pitts, J. N., Jr. *Chemistry of the Upper and Lower Atmosphere*; Academic Press: San Diego, 2000.

(2) Berresheim, H.; Wine, P. H.; Davis, D. D. *Composition, Chemistry, and Climate of the Atmosphere*; Singh, H. B., Ed.; Van Nostrand Reinhold: New York, 1995; p 268.

(3) Morokuma, K.; Muguruma, C. *J. Am. Chem. Soc.* **1994**, *116*, 10316.

(4) Lovejoy, E. R.; Hanson, D. R.; Huey, L. G. *J. Phys. Chem.* **1996**, *100*, 19911.

(5) Jayne, J. T.; Pöschl, U.; Chen, Y.-M.; Dai, D.; Molina, L. T.; Worsnop, D. R.; Kolb, C. E.; Molina, M. J. *J. Phys. Chem.* **1997**, *101*, 10000.

(6) Larson, L. J.; Kuno, M.; Tao, F.-M. *J. Chem. Phys.* **2000**, *112*, 8830.

(7) Lovejoy, E. R.; Hanson, D. R. *J. Phys. Chem.* **1996**, *100*, 4459.

(8) Seinfield, J. H. *Atmospheric Chemistry and Physics of Air Pollution*; Wiley: New York, 1986; p 738.

(9) Leopold, K. R.; Canagaratna, M.; Phillips, J. A. *Acc. Chem. Res.* **1997**, *30* (2), 57.

(10) Canagaratna, M.; Phillips, J. A.; Goodfriend, H.; Leopold, K. R. *J. Am. Chem. Soc.* **1996**, *118* (22), 5290.

(11) Leopold, K. R. *Adv. Mol. Struct. Res.* **1996**, *2*, 103.

(12) Hickling, S. J.; Woolley, R. G. *Chem. Phys. Lett.* **1990**, *166*, 43.

(13) Wong, M. W.; Wiberg, K. B.; Frisch, M. J. *J. Am. Chem. Soc.* **1992**, *114*, 523.

(14) Shen, G.; Suto, M.; Lee, L. C. *J. Geophys. Res.* **1990**, *95* (D9), 13981.

(15) Hoffmann, M.; Schleyer, P. v. R. *J. Am. Chem. Soc.* **1994**, *116*, 4947.

(16) Lovejoy, E. R. *J. Phys. Chem.* **1997**, *101*, 4950.

(17) Coffman, D. J.; Hegg, D. A. *J. Geophys. Res.* **1995**, *100*, 7147.

(18) Weber, R. J.; McMurry, P. H.; Eisle, F. L.; Tanner, D. J. *J. Atmos. Sci.* **1995**, *52*, 2242.

(19) Weber, R. J.; McMurry, P. H.; Mauldin, L.; Tanner, D. J.; Eisle, F. L.; Brechtel, F. J.; Kreidenweis, S. M.; Kok, G. L.; Schillawski, R. D.; Baumgardner, D. *J. Geophys. Res.* **1998**, *103*, 16385.

(20) Becke, A. D. *J. Chem. Phys.* **1992**, *96*, 2155.

(21) Becke, A. D. *J. Chem. Phys.* **1992**, *97*, 9193.

(22) Becke, A. D. *J. Chem. Phys.* **1993**, *98*, 5648.

(23) Lee, C.; Yang, W.; Parr, R. G. *Phys. Rev. B* **1988**, *37*, 785.

(24) Møller C.; Plesset, M. J. *Phy. Rev.* **1934**, *26*, 618.

(25) Brinkley, J. S.; Pople, J. A. *Int. J. Quantum Chem*. **1975**, *9*, 229.

(26) Kim, K.; Jordan, K. D. *J. Phys. Chem*. **1994**, *98*, 10089.

(27) Rablen, P. R.; Lockman, J. W.; Jorgensen, W. L. *J. Phys. Chem. A* **1998**, *102*, 3782.

(28) Cizek, J. *Adv. Chem. Phys*. **1969**, *14*, 35.

(29) Purvis, G. D.; Barlett, R. J. *J. Chem. Phys*. **1982**, *76*, 1910.

(30) Pople, J. A.; Head-Gordon, M.; Raghavachari, K. *J. Chem. Phys*. **1988**, *89*, 7382.

(31) Krishnan, R.; Brinkley, J. S.; Seeger R.; Pople, J. A. *J. Chem. Phys*. **1980**, *72*, 650.

(32) Frisch, M. J.; Pople, J. A.; Brinkley, J. S. *J. Chem. Phys*. **1984**, *80*, 3265.

(33) Clark, T.; Chandrasekhar, J.; Spitznagel, G. W.; Schleyer, P. v. R. *J. Comput. Chem*. **1983**, *4*, 294.

(34) Peng, C.; Schlegel, H. B. *Isr. J. Chem*. **1993**, *37*, 785.

(35) Gonzalez, C.; Schlegel, H. B. *J. Chem. Phys*. **1989**, *90*, 2154.

(36) Gonzalez, C.; Schlegel, H. B. *J. Phys. Chem*. **1990**, *94*, 5523.

(37) Hehre, W. J.; Random, L.; Schleyer, P. v. R.; Pople, J. A. *Ab Initio Molecular Orbital Theory*; Wiley: New York, 1986.

(38) Frisch, M. J.; Trucks, G. W.; Schlegel, H. B.; Scuseria, G. E.; Robb, M. A.; Cheeseman, J. R.; Zakrzewski, V. G.; Montgomery, J. A., Jr.; Stratmann, R. E.; Burant, J. C.; Dapprich, S.; Millam, J. M.; Daniels, A. D.; Kudin, K. N.; Strain, M. C.; Farkas, O.; Tomasi, J.; Barone, V.; Cossi, M.; Cammi, R.; Mennucci, B.; Pomelli, C.; Adamo, C.; Clifford, S.; Ochterski, J.; Petersson, G. A.; Ayala, P. Y.; Cui, Q.; Morokuma, K.; Malick, D. K.; Rabuck, A. D.; Raghavachari, K.; Foresman, J. B.; Cioslowski, J.; Ortiz, J. V.; Stefanov, B. B.; Liu, G.; Liashenko, A.; Piskorz, P.; Komaromi, I.; Gomperts, R.; Martin, R. L.; Fox, D. J.; Keith, T.; Al-Laham, M. A.; Peng, C. Y.; Nanayakkara, A.; Gonzalez, C.; Challacombe, M.; Gill, P. M. W.; Johnson, B.; Chen, W.; Wong, M. W.; Andres, J. L.; Gonzalez, C.; Head-Gordon, M.; Replogle, E. S.; Pople, J. A. *Gaussian 98*, Revision A.2; Gaussian Inc.: Pittsburgh, PA, 1998.

(39) Werner, H.-J.; Knowles, P. J.; with contributions from Amos, R. D.; Berning, A.; Cooper, D. L.; Deegan, M. J. O.; Dobbyn, A. J.; Eckert, F.; Hampel, C.; Hetzer, G.; Leininger, T.; Lindh, R.; Lloyd, A. W.; Meyer, W.; Mura, M. E.; Nicklass, A.; Palmieri, P.; Peterson, K.; Pitzer, R.; Pulay, P.; Rauhut, G.; Schütz, M.; Stoll, H.; Stone A. J.; Thorsteinsson, T. MOLPRO version 2000.1; University of Birmingham: Birmingham, 1999.

(40) Phillips, J. A.; Canagaratna, M.; Goodfriend, H.; Leopold, K. R. *J. Phys. Chem*. **1995**, *99*, 501.

(41) Larson, L. J.; Largent, A.; Tao, F-.M. *J. Phys. Chem. A* **1999**, *103*, 6786.

(42) Shi, Z.; Ford, J. V.; Castleman, A. W., Jr. *Chem. Phys. Lett*. **1994**, *220*, 274.